Spectral band difference effects on radiometric cross-calibration between multiple satellite sensors in the Landsat solar-reflective spectral domain

P.M. Teillet [*] [a], G. Fedosejevs [a], and K.J. Thome [b]

[a] Canada Centre for Remote Sensing, 588 Booth Street, Ottawa, Ontario, K1A 0Y7
[b] Remote Sensing Group, Optical Sciences Center, University of Arizona,
1630 E. University Blvd, Tucson, Arizona, USA 85721-0094

ABSTRACT

This paper reports on an investigation of radiometric calibration errors due to differences in spectral response functions between satellite sensors when attempting cross-calibration based on near-simultaneous imaging of common ground targets in analogous spectral bands. Five Earth observation sensors on three satellite platforms were included on the basis of their overpass times being within 45 minutes of each other on the same day (Landsat-7 ETM+; EO-1 ALI; Terra MODIS; Terra ASTER; Terra MISR). The simulation study encompassed spectral band difference effects (SBDE) on cross-calibration between all combinations of the sensors considered, using the Landsat solar reflective spectral domain as a framework. Scene content was simulated using ground target spectra for the calibration test sites at Railroad Valley Playa, Nevada and Niobrara Grassland, Nebraska. Results were obtained as a function of calibration test site, satellite sensor, and spectral region. Overall, in the absence of corrections for SBDE, the Railroad Valley Playa site is a "good" to "very good" ground target for cross-calibration between most but not all satellite sensors considered in most but not all spectral regions investigated. "Good" and "very good" are defined as SBDEs within +/- 3 % and +/- 1 %, respectively. Without SBDE corrections, the Niobrara test site is only "good" for cross-calibration between certain sensor combinations in some spectral regions. The paper includes recommendations for spectral data and tools that would facilitate cross-calibration between multiple satellite sensors.

Keywords: spectral response functions, radiometric calibration, satellite sensors, optical remote sensing.

1. INTRODUCTION

In order for quantitative Earth observation applications to make full use of the ever-increasing number of Earth observation satellite systems, data from the various sensors involved must be on a consistent radiometric calibration scale. However, different applications and technology developments in Earth observation typically require different spectral coverage. The result is that relative spectral response functions differ significantly between sensors, even for spectral bands designed to look at the same region of the electromagnetic spectrum. While it would be advantageous to have satellite sensors with at least a small subset of standardized spectral bands in common[1], the technical feasibility of such an initiative would have to be addressed. As for the financial feasibility, any additional cost to achieve such standardization would, arguably, be more than recovered by savings in user efforts required to standardize data sets after satellite data acquisition. At the very least, a systematic attempt should be made to ensure that the main optical calibration test sites around the world are fully characterized spectrally with respect to their surface and atmospheric conditions[2, 3, 4].

Earth surfaces with suitable characteristics have long been used for the post-launch radiometric calibration of satellite sensors, usually referred to as vicarious or ground-look calibration[5, 6]. Reflectance-based or radiance-based methods use

[*] phil.teillet@ccrs.nrcan.gc.ca; phone 1-613-947-1251; fax 1-613-947-1408; http://www.ccrs.nrcan.gc.ca/ccrs/

Sensors, Systems, and Next-Generation Satellites VIII, edited by Roland Meynart, Steven P. Neeck, Haruhisa Shimoda, Proceedings of SPIE Vol. 5570
(SPIE, Bellingham, WA, 2004) · 0277-786X/04/$15 doi: 10.1117/12.562709

surface measurements to estimate top-of-atmosphere radiance at the entrance aperture of a given satellite sensor in order to provide an update of the nominal sensor calibration and to serve as a check on sensor performance over time. Traditionally, field measurement campaigns at such test sites have targeted only one or two sensors per sortie. More recently, with the increase in the number of sensors that pass over a test site on a given day, it has become possible with careful planning by specialised teams to undertake ground-look calibrations for several sensors per sortie[7]. Nevertheless, efforts such as these remain resource intensive and, hence, it is of considerable interest to develop less expensive complementary approaches that can provide more frequent calibration updates, even if they are less accurate. The use of test sites to transfer radiometric calibration between satellite sensors has also been on the increase, with and without coincident surface measurements. With cost reductions in mind, methods that yield useful results without near-simultaneous measurements by field crews[8, 9] and/or that take advantage of autonomous in-situ sensors[3] need to be explored.

1.1 Previous studies on cross-calibration

Teillet et al.[9] reported on a radiometric cross-calibration of the Landsat-7 Enhanced Thematic Mapper Plus (ETM+) and Landsat-5 Thematic Mapper (TM) sensors based on tandem-orbit data sets. The methodology incorporated adjustments for spectral band differences between the two Landsat sensors. Spectral band difference effects (SBDE) were shown to be significant, despite the close similarity in spectral filters and response functions, and more dependent on the surface reflectance spectrum than on atmospheric and illumination conditions. A variety of terrestrial surfaces were assessed regarding their suitability for Landsat radiometric cross-calibration in the absence of surface reflectance spectra.

Trishchenko et al.[10] focused on moderate resolution satellite sensors, including the Advanced Very High Resolution Radiometers (AVHRR) onboard the NOAA-6, -7, -8, -10, -11, -12, -14, -15, -16 spacecraft, Terra Moderate-resolution Imaging Spectroradiometer (MODIS), SPOT-4 Vegetation (VGT), and Global Imager (GLI) on the second Advanced Earth Observing Satellite (ADEOS-2), all with respect to NOAA-9 AVHRR. They reported on modeling results in the red and near infrared (NIR) and also emphasized the effect of spectral band differences on the Normalized Difference Vegetation Index (NDVI), the most widely used index for vegetation monitoring. They also reported that, in the absence of corrections for spectral band differences, reflectance differences range from –25 % to +12 % in the red and –2 % to +4 % in the NIR, even between "same type" AVHRR sensors, and that still greater differences can arise for the other sensor inter-comparisons. NDVI differences were found to range from –0.02 to +0.06.

Steven et al.[11] provided additional background on the problem of inter-calibrating vegetation indices and reported on a simulation study involving red and NIR spectral bands and vegetation indices for 15 satellite sensors. Surface spectral reflectance measurements of agricultural targets were used to generate the results. Conversion coefficients were generated for all sensor combinations and were found to enable inter-sensor NDVI comparisons to a precision of 2 %.

Rao et al.[8] presented results on the inter-calibration of Terra MODIS and the European Remote Sensing satellite-2 (ERS-2) Along-Track Scanning Radiometer-2 (ATSR-2) based on desert sites as common targets. They emphasized how crucial it is to take into consideration the spectral character of the sensors and the scene to avoid compromising the efficacy of inter-calibration.

To recap, previous studies on cross-calibration have looked at calibration continuity between two Landsat sensors and inter-comparisons of NDVI derived from many sensors for vegetation monitoring. The role of the spectral dimension in cross-calibration has been taken into account directly or indirectly in these studies. The investigation described in this paper focuses on two test sites frequently used for the vicarious calibration of individual sensors and encompasses the full Landsat solar-reflective spectral domain for cross-calibrations between five sensors that provide near-simultaneous imaging of the Earth.

1.2 Study premise

This paper reports on an investigation of radiometric calibration errors due to differences in spectral response functions between satellite sensors when attempting cross-calibration (Xcal) based on near-simultaneous imaging of common ground targets in analogous spectral bands. In particular, the study assesses the magnitude of SBDEs and their impact on cross-calibration if they are not or cannot be taken into account. Adequate SBDE corrections may not be possible in the absence of surface spectral measurements or they may be approximate if historical spectra are used that are not necessarily representative of the test site on the satellite-imaging day.

Given that the Landsat-7 ETM+ is well-calibrated radiometrically, cross-calibration between the ETM+ and several other sensors was the starting point for the study. With SBDEs on cross calibration between ETM+ and other sensors in hand, it was straightforward to examine all other combinations between sensors (in spectral bands with analogs to one or more of the six solar-reflective Landsat bands). In particular, five Earth observation sensors on three satellite platforms were included on the basis of their overpass times being within 45 minutes of each other on the same day (Landsat-7 ETM+; Earth Observing-1 Advanced Land Imager (EO-1 ALI); Terra MODIS; Terra Advanced Spaceborne Thermal Emission and Reflection (ASTER); Terra Multi-angle Imaging Spectro-Radiometer (MISR)). Scene content was simulated using ground target spectra for the calibration test sites at Railroad Valley Playa, Nevada and Niobrara Grassland, Nebraska. Results were obtained as a function of calibration test site, satellite sensor, and spectral region. The paper also makes recommendations on spectral data and tools that would facilitate cross-calibration between multiple satellite sensors.

1.3 Assumptions

Temporal and spatial:

- As already noted, this work concerns spectral response effects on radiometric cross-calibration between satellite sensors that have imaged common ground targets within a short space of time. Ideally, "a short space of time" in this context implies within minutes in order to avoid variable solar illumination and atmospheric conditions. In practice, calibration data sets are typically acquired on very clear days and so same-day comparisons are acceptable within a framework of systematic monitoring of sensor calibration performance. Attempts to cross-calibrate multiple satellite sensors imaging a test site one or more days apart can yield mixed results[2]. Thus, it is assumed that the images to be used for cross-calibration between sensors are acquired under clear sky conditions on the same day. Cross-calibration methodologies can be designed to avoid susceptibility to possible spatial misregistration of multiple images of common ground targets[9].

Spectral:

- Radiometric cross-calibration between the five satellite sensors is undertaken in spectral bands with analogs to the six solar-reflective Landsat-7 ETM+ bands (Table 1, Figure 1). There may some day be a better set of spectral bands on a satellite sensor to use for this purpose, but for now the Landsat-centric perspective is used.
- It is assumed that the spectral bands were well characterized prior to launch and that they remain unchanged post-launch. Few investigations have addressed the impact of post-launch changes in spectral band characteristics[12, 3, 14]. Once a given satellite sensor is in orbit, it is difficult to assess changes in the sensor's spectral characteristics. An exception is the Terra MODIS, which includes a sub-system called the Spectroradiometric Calibration Assembly (SRCA). The SRCA confirms that the MODIS spectral bands have not changed significantly since launch[15]. With today's ion-assisted deposition filters, satellite sensor spectral bands are much less prone to post-launch degradation.
- Out-of-band response is not taken into consideration. Even almost identical spectral bands being compared can have significantly different out-of-band response between sensors (John L. Barker, personal communication).

Satellite	Sensor	Blue Band	Green Band	Red Band	NIR Band	SWIR Band I	SWIR Band II
Landsat-7	ETM+	1	2	3	4	5	7
Earth Observing 1	ALI	1	2	3	4p	5	7
Terra	MODIS	3	4	1	2	6	7
Terra	MODIS	10	12	13	16	-	-
Terra	ASTER	-	1	2	3	4	6
Terra	MISR	1	2	3	4	-	-

Table 1. Satellite sensors and analogous spectral band numbers, where NIR = near infrared; SWIR = shortwave-infrared. Figure 1 illustrates the spectral response profiles for all satellite sensors in the green and SWIR band I spectral domains as examples.

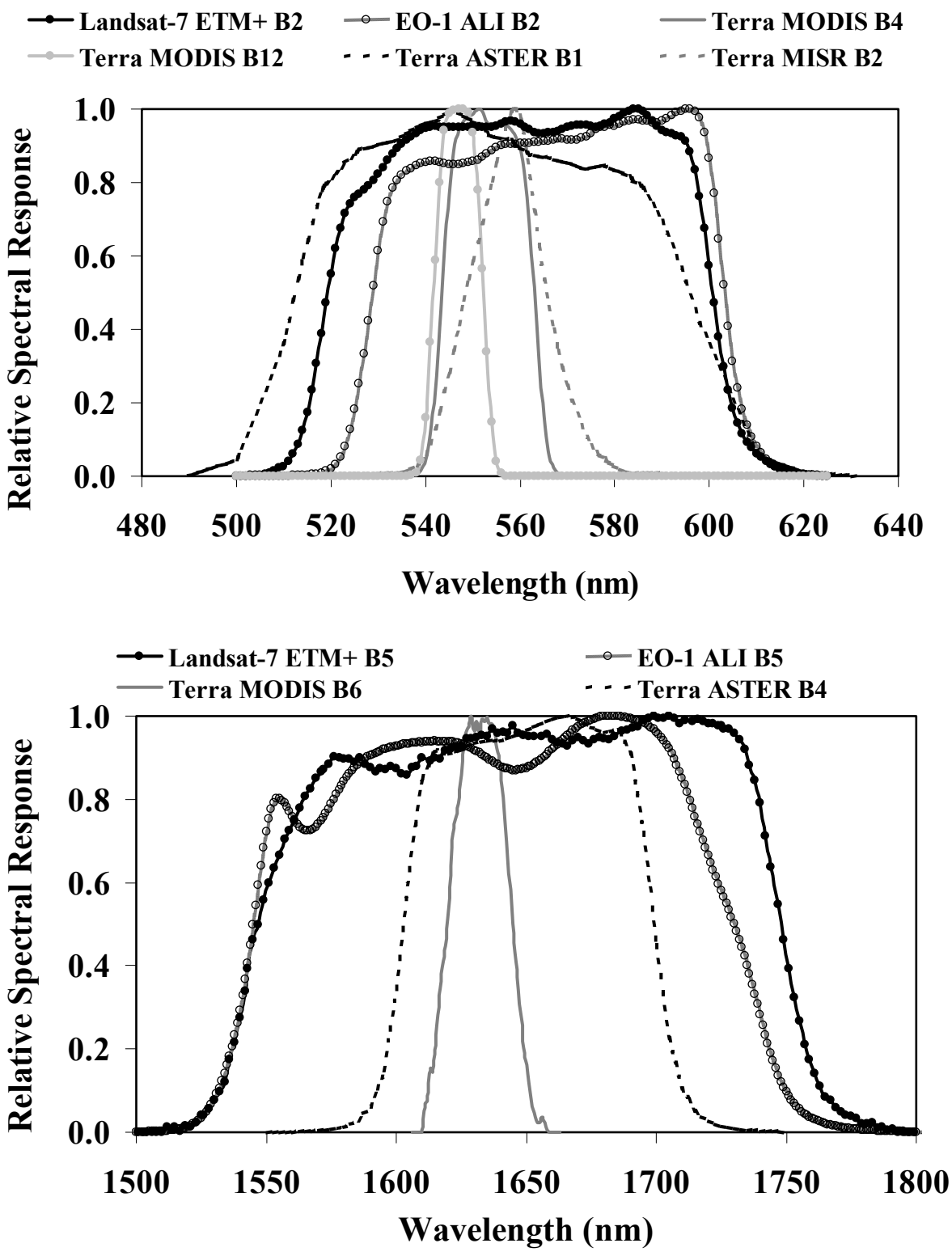

Figure 1. Satellite sensor spectral bands analogous to Landsat ETM+ band 2 (top) and band 5 (bottom).

Radiometric:

- It is assumed that the satellite sensors under consideration have linear radiometric response over the range of relevant radiances.
- Differences in radiometric resolution were not taken into consideration.
- The first phase of this study, reported in this paper, considered only one atmospheric aerosol optical depth (0.05 at 0.55 micrometers), one solar zenith angle (60 degrees) and nadir viewing geometry. An aerosol optical depth on the order of 0.05 at 0.55 micrometers can be considered typical for clear days where continental aerosols prevail[4, 16]. Results for different aerosol optical depths and different solar zenith and viewing angles will be generated in the next phase of the work. Indications from Teillet et al.[9] are that SBDEs are more dependent on the surface reflectance spectrum than on atmospheric and illumination conditions.
- Bidirectional reflectance effects were not taken into account.
- The terrain is assumed to be flat and horizontal, a good assumption for the test sites considered.

2. RADIOMETRIC FORMULATION

The key radiometric equations for at-sensor quantities are as follows[9]. For a given spectral band i:

$$\text{Image quantized level (in counts)} = Q_i = G_i L^*_i + Q_{0i} \quad , \tag{1}$$

$$\text{At-sensor radiance (in Watts/(m}^2 \text{ sr } \mu\text{m))} = L^*_i = (Q_i - Q_{0i}) / G_i = \Delta Q_i / G_i \quad , \tag{2}$$

$$\text{At-sensor reflectance} = \rho^*_i = \pi L^*_i d_s^2 / (E_{0i} \cos\theta) \quad . \tag{3}$$

In these equations, G_i is band-averaged sensor responsivity (in counts per unit radiance) and Q_{0i} is the zero-radiance bias (in counts) in spectral band i. Also, E_{0i} is the exo-atmospheric solar irradiance (in Watts/(m^2 μm)), θ is the solar zenith angle, and d_s is the Earth-Sun distance in Astronomical Units. Bias-corrected image values are then given by

$$\Delta Q_i = Q_i - Q_{0i} = G_i \rho^*_i E_{0i} \cos\theta / (\pi d_s^2) \quad . \tag{4}$$

There are two advantages to using reflectances instead of radiances. One advantage is to allow for the cosine effect of different solar zenith angles due to the time difference between data acquisitions. The other advantage is to compensate for different exo-atmospheric solar irradiances arising from spectral band differences. If differences in atmospheric conditions are not a factor, then the top-of-atmosphere (TOA) at-sensor reflectance comparisons have the potential to yield the best possible calibration comparisons between multiple sensors based on common ground looks.

Cross-calibration methodologies in general should consider adjustments as appropriate for bi-directional reflectance factor effects due to differences in illumination and observation angles. Even if the same test sites are imaged the same day, significant overpass time and off-nadir viewing geometry differences can arise depending on the satellite sensor.

2.1. Cross-calibration for raw data

Radiometric calibration specialists often use raw (Level-0) data and seek to update responsivity coefficients for the sensors under consideration. The following formulation is developed accordingly. Equation (4) can be defined separately for image data from a reference sensor ("R") and for image data from another sensor ("X"), whose calibration is to be checked via cross-calibration with respect to sensor R in analogous spectral band i. After algebraic manipulation, this leads to a cross-calibration between image data from sensor R and adjusted image data from sensor X:

$$\Delta Q_{iXA} = A_i \Delta Q_{iX} = (G_{iX} / G_{iR}) \Delta Q_{iR} = M_i \Delta Q_{iR} \quad , \tag{5}$$

where the factor A_i adjusts sensor X radiances for illumination and spectral band difference effects and M_i is the slope of the linear equation that characterizes ΔQ_{iXA} as a function of ΔQ_{iR}. In particular,

$$A_i = B_i (E_{0i} \cos\theta)_R / (E_{0i} \cos\theta)_X \quad , \tag{6}$$

where

$$B_i = \rho^*_{iR} / \rho^*_{iX} \quad . \tag{7}$$

B_i is essentially a spectral band adjustment factor, given that ρ^*_{iX} and ρ^*_{iR} are not the same because of the differences in relative spectral response profiles between corresponding (analogous) spectral bands. Figure 1 illustrates these differences for the green band and a shortwave infrared band for the satellite sensors involved. Sensor X responsivity G_{iX} in spectral band i is then given (in counts per unit radiance) by

$$G_{iX} = M_i G_{iR} \quad . \tag{8}$$

Thus, one of the keys to this method of cross-calibration is to have sufficient knowledge of the spectral band adjustment factor B_i , since uncertainty in the cross-calibration due to this effect is directly proportional to the uncertainty in B_i .

3. METHODOLOGY

3.1. Ground targets

The test sites at Railroad Valley Playa, Nevada (RVPN) and Niobrara Grassland, Nebraska (NIOB) were used because surface spectral reflectance data were available (Figure 2). The spectra were obtained using portable Analytical Spectral Devices (ASD) spectrometers (the NIOB spectrum was kindly provided by Scott E. Black and Dennis L. Helder, South Dakota State University). Figure 3 shows the portions of the surface reflectance spectra for the two test sites that are in the Landsat ETM+ band 2 and band 5 spectral regions.

The RVPN test site is a dry-lake playa that is very homogeneous and consists of compacted clay-rich lacustrine deposits forming a relatively smooth surface compared to most land covers. The NIOB test site is characterized primarily by grasslands grazed by cattle and by a smaller proportion of agricultural crops. Both test sites have been used for ground-look calibration of satellite sensors and RVPN in particular is one of the most extensively characterised and used optical calibration test sites in the world.

3.2. Generation of spectral band adjustment factors

The key parameter to be computed is the spectral band adjustment factor B_i (equation (7)) in a given spectral band i (Table 1), which is a function of TOA reflectances. The surface reflectance spectra for both ground targets were used as inputs to an atmospheric radiative transfer (RT) code to calculate the TOA reflectances in corresponding solar reflective spectral bands for all five sensors under consideration.

The RT code is the Canadian Advanced Modified 5S (CAM5S) code[17]. Inputs consisted of the aforementioned surface reflectance spectra plus standard choices for the atmospheric models (US62 atmospheric profile and continental aerosol model). The aerosol optical depth was set at 0.05 at 0.55 micrometers and the solar zenith angle was set at 60 degrees. An Earth-Sun distance of 1 A.U. and nadir viewing geometry were also assumed. Actual terrain elevations were used (1.425 km and 0.760 km for RVPN and NIOB, respectively).

3.3. Normalized difference vegetation index (NDVI)

Given that the NIOB test site is a grassland area, it is meaningful to generate results for NDVI, which can be defined as a function of TOA reflectance in the red and NIR bands as follows.

$$NDVI = (\rho^*_{NIR} - \rho^*_{red}) / (\rho^*_{NIR} + \rho^*_{red}) . \quad (9)$$

Analogous to the Bi factors (equation (7)), the SBDE on the comparison of NDVI obtained from sensors X and R is defined as the ratio

$$B_N = NDVI_R / NDVI_X . \quad (10)$$

TOA-based results were deemed to be sufficient to assess the magnitude of the SBDE, even though some users define NDVI as a function of surface reflectances.

4. RESULTS

The modeling results are presented in the form of matrices of the spectral band adjustment factors B_i for all sensor spectral band combinations for both test sites (Table 2). Because SBDEs are but one of many sources of sensor Xcal uncertainty, one would like them to be as small as possible. Hence, "very good" cases are considered to be those where the spectral band adjustment factors (B_i = ratio of TOA reflectance for sensor R / TOA reflectance for sensor X) are within ± 1 % of $B_i = 1$ (i.e., 0.99 – 1.01). In such cases, uncertainty or lack of knowledge about the spectral content of the scene should not significantly compromise the cross-calibration. Similarly, "good" results are defined as those that are ± 1 % to 3 % off $B_i = 1$ (i.e., in the range of 0.97-0.99 and 1.01-1.03), whereas "poor" results are those off by ± 3 % to 7 % (i.e., in the ranges of 0.93-0.97 and 1.03-1.07). "Bad" cases are those with spectral adjustment factors off by greater than 7 % (i.e., in the ranges of < 0.93 and > 1.07).

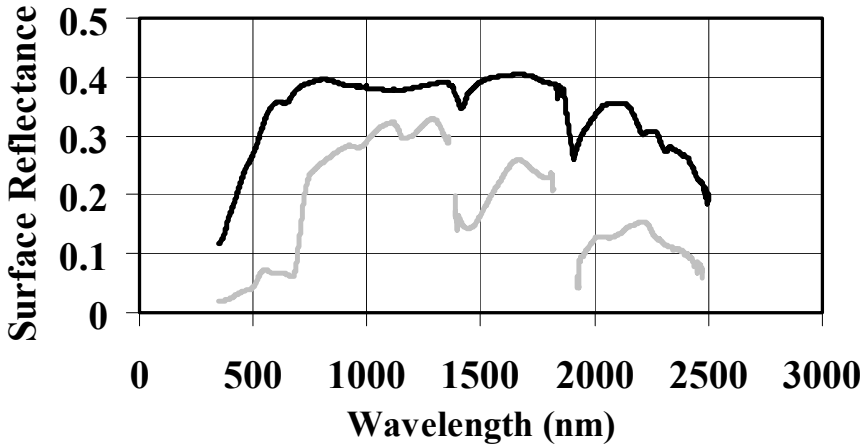

Figure 2. Surface reflectance spectra derived from ASD measurements at Railroad Valley Playa on June 1, 1999 (black curve) and at Niobrara on June 2, 1999 (grey curve).

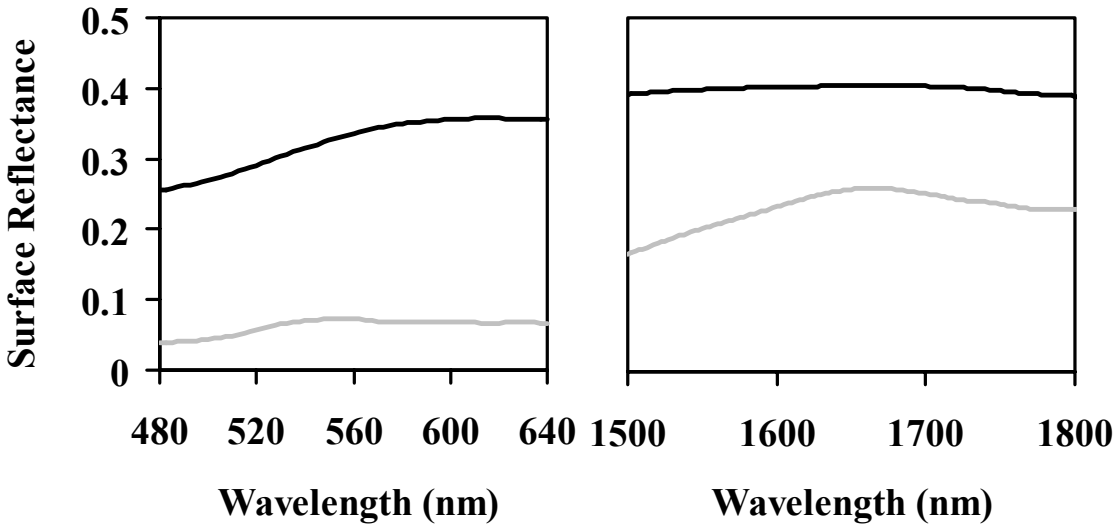

Figure 3. Portions of surface reflectance spectra in Figure 2 for Railroad Valley Playa (black curve) and Niobrara (grey curve) that are in the Landsat ETM+ band 2 and band 5 spectral ranges.

It is clear from Table 2 that the RVPN calibration site is less susceptible to SBDEs than the NIOB site in almost all sensor Xcal combinations examined. For the NIOB site and for the sensors involved, with few exceptions, the spectral content of the scene must be known for accurate cross-calibration based on near-simultaneous imaging.

The green spectral region for the RVPN site is the best overall in that two-thirds of the Xcal combinations are "very good' and the remaining third are all "good". The "poorest" spectral region overall is the NIR for both test sites. For the NIOB site, there are no spectral regions that can be considered "very good" and only the green and red spectral regions have more than a few "good" Xcal combinations. For the RVPN site, the ETM+ band 7 analog spectral region is also to be avoided in the absence of SBDE corrections.

Sensor Spectral Bands	RailroadValley Playa						Niobrara Grassland					
ETM+ Band 1 Analogs	**A**	**B**	**C**	**D**	**E**	**F**	**A**	**B**	**C**	**D**	**E**	**F**
A: Landsat-7 ETM+ B1	1	0.995		1.005	0.990	1.025	1	1.032		0.967	1.076	0.844
B: EO-1 ALI B1		1		1.010	0.995	1.030		1		0.937	1.043	0.818
C: Terra ASTER N/A												
D: Terra MODIS B3				1	0.985	1.020				1	1.113	0.873
E: Terra MODIS B10					1	1.035					1	0.784
F: Terra MISR B1						1						1
ETM+ Band 2 Analogs	**A**	**B**	**C**	**D**	**E**	**F**	**A**	**B**	**C**	**D**	**E**	**F**
A: Landsat-7 ETM+ B2	1	0.996	1.005	0.990	0.988	0.989	1	1.018	0.982	0.956	1.005	0.966
B: EO-1 ALI B2		1	1.009	0.994	0.992	0.993		1	0.965	0.939	0.987	0.949
C: Terra ASTER B1			1	0.985	0.983	0.984			1	0.974	1.023	0.984
D: Terra MODIS B4				1	0.998	0.999				1	1.051	1.010
E: Terra MODIS B12					1	1.001					1	0.961
F: Terra MISR B2						1						1
ETM+ Band 3 Analogs	**A**	**B**	**C**	**D**	**E**	**F**	**A**	**B**	**C**	**D**	**E**	**F**
A: Landsat-7 ETM+ B3	1	0.998	1.001	0.997	1.016	0.950	1	1.004	0.962	0.983	1.017	1.015
B: EO-1 ALI B3		1	1.003	0.999	1.018	0.952		1	0.958	0.979	1.013	1.011
C: Terra ASTER B2			1	0.996	1.015	0.949			1	1.022	1.057	1.055
D: Terra MODIS B1				1	1.019	0.953				1	1.035	1.033
E: Terra MODIS B13					1	0.935					1	0.998
F: Terra MISR B3						1						1
ETM+ Band 4 Analogs	**A**	**B**	**C**	**D**	**E**	**F**	**A**	**B**	**C**	**D**	**E**	**F**
A: Landsat-7 ETM+ B4	1	0.947	1.037	0.961	0.942	0.948	1	0.911	1.069	0.926	0.906	0.911
B: EO-1 ALI B4p		1	1.095	1.015	0.995	1.001		1	1.173	1.016	0.995	1.000
C: Terra ASTER B3			1	0.927	0.908	0.914			1	0.866	0.848	0.852
D: Terra MODIS B2				1	0.980	0.986				1	0.978	0.984
E: Terra MODIS B16					1	1.006					1	1.006
F: Terra MISR B4						1						1
ETM+ Band 5 Analogs	**A**	**B**	**C**	**D**	**E**	**F**	**A**	**B**	**C**	**D**	**E**	**F**
A: Landsat-7 ETM+ B5	1	0.989	0.976	0.972			1	0.992	0.931	0.920		
B: EO-1 ALI B5		1	0.987	0.983				1	0.939	0.927		
C: Terra ASTER B4			1	0.996					1	0.988		
D: Terra MODIS B6				1						1		
E: Terra MODIS N/A												
F: Terra MISR N/A												
ETM+ Band 7 Analogs	**A**	**B**	**C**	**D**	**E**	**F**	**A**	**B**	**C**	**D**	**E**	**F**
A: Landsat-7 ETM+ B7	1	0.957	0.938	0.795			1	0.947	0.804	0.846		
B: EO-1 ALI B7		1	0.980	0.831				1	0.849	0.893		
C: Terra ASTER B6			1	0.848					1	1.052		
D: Terra MODIS B7				1						1		
E: Terra MODIS N/A												
F: Terra MISR N/A												

Table 2. Results for spectral band adjustment factors B_i. Relative to $B_i = 1$, cells for factors within ± 1 % (i.e., 0.99 – 1.01) are white, factors within ± 1 % to 3 % (i.e., 0.97-0.99 and 1.01-1.03) are light grey, factors within ± 3 % to 7 % (i.e., 0.93-0.97 and 1.03-1.07) are medium grey, and factors greater than 7 % (i.e., < 0.93 and > 1.07) are dark grey.

Sensor Xcal combinations involving ETM+, ALI, ASTER and one MODIS band set (bands 3, 4, and 1) are "very good" in the blue, green and red spectral regions for RVPN (the one exception is the band 2 analog band combination of ASTER band 1 and MODIS band 4 where $B_i = 0.985$). Sensor combinations involving MISR are the most susceptible to SBDEs, with generally "poor" results. Overall, there are no sensor Xcal combinations for which the entire Landsat solar-reflective spectral domain yields "good" results in the absence of SBDE corrections.

While there are a few "very good" cases, overall the NDVI is highly susceptible to SBDEs (Table 3), with a percent root mean square difference in B_N (equation 10) from unity of 9.4 % across the set of 15 comparisons.

Sensor	Niobrara Grassland					
ETM+ NDVI Analogs	**A**	**B**	**C**	**D**	**E**	**F**
A: Landsat-7 ETM+	**1**	**1.068**	**0.923**	**1.080**	**1.080**	**1.076**
B: EO-1 ALI		**1**	**0.864**	**1.011**	**1.011**	**1.007**
C: Terra ASTER			**1**	**1.170**	**1.170**	**1.166**
D: Terra MODIS B1B2				**1**	**1.000**	**0.996**
E: Terra MODIS B13B16					**1**	**0.996**
F: Terra MISR						**1**

Table 3. Results for spectral band effects on NDVI B_N. Relative to $B_N = 1$, cells for factors within ± 1 % (i.e., 0.99 – 1.01) are white, factors within ± 1 % to 3 % (i.e., 0.97-0.99 and 1.01-1.03) are light grey, factors within ± 3 % to 7 % (i.e., 0.93-0.97 and 1.03-1.07) are medium grey, and factors greater than 7 % (i.e., < 0.93 and > 1.07) are dark grey.

5. CONCLUDING REMARKS

Spectral band difference effects (SBDE) have been investigated in the context of radiometric cross-calibration (Xcal) between multiple satellite sensors in the Landsat solar-reflective spectral domain. The modeling results are presented in the form of spectral band adjustment factors for all sensor spectral band combinations for two test sites. The results were assessed with stringent uncertainty requirements in mind and considered to be "very good" only for spectral band adjustment factors within ± 1 % of unity or "good" for factors within ± 1 % to 3 %.

It is clear from the results that, except for a limited number of cases, sound Xcal requires that the spectral characteristics of the common ground targets used be known. Indeed, even for the Railroad Valley Playa test site, a target that has relatively low spectral variability across most wavelength regions of interest, one can only do without SBDE corrections in selected cases: primarily sensor Xcal combinations involving ETM+, ALI, ASTER, and MODIS in the blue, green, and red spectral regions. Thus, low-cost Xcal methodologies that seek to complement the more accurate calibrations that often (but not always) result from costly field campaigns should somehow take SBDEs into account.

The following spectral data and tools are recommended to facilitate cross-calibration between satellite sensors.

- An on-line repository of relative spectral response profiles for as many Earth observation sensors as possible.
- An on-line repository of well-documented ground spectra for key calibration test sites.
- Tools for easy transformations between different wavelength grids to facilitate comparisons.

Agencies that assume responsibility for one or more of these repositories should coordinate their activities with the Committee on Earth Observation Satellites (CEOS) Working Group on Calibration and Validation (WGCV).

REFERENCES

1. Teillet, P.M., Horler, D.N.H., and O'Neill, N.T., "Calibration/Validation, Stability Monitoring, and Quality Assurance in Remote Sensing: A New Paradigm". *Canadian Journal of Remote Sensing*, **23(4)**: 401-414 (1997).

2. Teillet, P.M., Fedosejevs, G., Gauthier, R.P., O'Neill, N.T., Thome, K.J., Biggar, S.F., Ripley, H., and Meygret, A., "A Generalized Approach to the Vicarious Calibration of Multiple Earth Observation Sensors Using Hyperspectral Data". *Remote Sensing of Environment*, **77(3)**: 304-327 (2000).

3. Teillet, P.M., Thome, K.J., Fox, N., and Morisette, J.T., "Earth Observation Sensor Calibration Using A Global Instrumented and Automated Network of Test Sites (GIANTS)", *Proceedings of SPIE Conference 4550 on Sensors, Systems, and Next-Generation Satellites V*, Toulouse, France, Eds. H. Fujisada, J.B. Lurie, and K. Weber, SPIE Volume **4550**, pp. 246-254 (2001).

4. Ahern, F.J., Gauthier, R.P., Teillet, P.M., Sirois, J., Fedosejevs, G., and Lorente, D., "An Investigation of Continental Aerosols with High Spectral Resolution Solar Extinction Measurements". *Applied Optics*, **30(36)**: 5276-5287 (1991).

5. Thome, K.J., "Absolute Radiometric Calibration of Landsat 7 ETM+ Using the Reflectance-Based Method". *Remote Sensing of Environment,* **78(1-2)**: 27-38 (2001).

6. Thome, K. J., Crowther, B.G., and Biggar, S.F., "Reflectance- and Irradiance-Based Calibration of Landsat-5 Thematic Mapper". *Canadian Journal of Remote Sensing,* **23**: 309-317 (1997).

7. Thome, K.J., Biggar, S.F., and Wisniewski, W., "Cross comparison of EO-1 sensors and other Earth resources sensors to Landsat-7 ETM+ using Railroad Valley Playa". *IEEE Transactions on Geoscience and Remote Sensing,* **41(6)**: 1180-1188 (2003).

8. Rao, C.R.N., Cao, C., and Zhang, N., "Inter-calibration of the Moderate-Resolution Imaging Spectroradiometer and the Along-Track Scanning Radiometer-2". *International Journal of Remote Sensing,* **24(9)**: 1913-1924 (2003).

9. Teillet, P. M., Barker, J., Markham, B. L., Irish, R. R., Fedosejevs, G., and Storey, J. C., "Radiometric Cross-Calibration of the Landsat-7 ETM+ and Landsat-5 TM Sensors Based on Tandem Data Sets". *Remote Sensing of Environment,* **78**: 39-54 (2001).

10. Trishchenko, A. P., Cihlar, J., and Li, Z., "Effects of Spectral Response Function on Surface Reflectance and NDVI Measured with Moderate Resolution Satellite Sensors". *Remote Sensing of Environment,* **81(1)**: 1-18 (2002).

11. Steven, M.D., Malthus, T.J., Baret, F., Xu, H., and Chopping, M.J., "Intercalibration of vegetation indices from different sensor systems". *Remote Sensing of Environment,* **88**: 412-422 (2003).

12. Flittner, D.E., and Slater, P.N., "Stability of Narrow-Band Filter Radiometers in the Solar-Reflective Range". *Photogrammetric Engineering and Remote Sensing*, **57(2)**: 165-171 (1991).

13. Teillet, P.M., "Effects of Spectral Shifts on Sensor Response". *Proceedings of the ISPRS Commission VII Symposium*, Victoria, B.C., pp. 59-65 (1990).

14. Suits, G.H., Malila, W.A., and Weller, T.M., "The Prospects for Detecting Spectral Shifts Due to Satellite Sensor Ageing". *Remote Sensing of Environment,* **26**: 17-29 (1988).

15. Che, N., Xiong, X., and Barnes, W., "On-Orbit Spectral Characterization Results for Terra MODIS Reflective Solar Bands". *Proceedings of SPIE Conference 5151 on Sensors, Systems, and Next-Generation Satellites,* San Diego, California, SPIE Volume **5151**, pp. 367-374 (2003).

16. Fedosejevs, G., O'Neill, N.T., Royer, A., Teillet, P.M., Bokoye, A.I., and McArthur, B., "Aerosol Optical Depth for Atmospheric Correction of AVHRR Composite Data". *Canadian Journal of Remote Sensing*, **26(4)**: 273-284 (2000).

17. O'Neill, N.T., Royer, A., and Nguyen, M.N., "Scientific and Technical Report on the Development of a Modified Version of the H5S Code which Incorporates Major Features of the 6S Code", CARTEL Internal Report CARTEL-1996-020, CARTEL, Department de géographie et télédétection, 2500, boul. de l'Université, Université de Sherbrooke, Sherbrooke, Québec, Canada J1K 2R1, 62 p (1996).